From Viscous Fingering to Viscoelastic Fracturing in Colloidal Fluids

E. Lemaire,[1] P. Levitz,[1] G. Daccord,[2] and H. Van Damme[1],[a]
[1]*CRMD, Centre National de la Recherche Scientifique and Université d'Orléans, 45071 Orléans CEDEX 02, France*
[2]*Dowell Schlumberger, BP 90, 42003 Saint Etienne CEDEX 1, France*
(Received 30 March 1990)

Fluid-displacement experiments in Hele-Shaw cells filled with a viscoelastic fluid show a novel transition between a viscous fingering (VF) regime producing fractal patterns of "fingers" and a viscoelastic fracturing (VEF) regime producing fractal patterns of "cracks." VEF patterns are characterized by branching angles of 90° with respect to the main crack, behind the tip, and by a lower fractal dimension than VF. The transition is controlled by several parameters, including the Deborah number and the system deformability.

PACS numbers: 46.30.Jv, 47.90.+a

The intrusion under pressure of a liquid into another phase may lead either to "viscous fingering" (VF) when a high-viscosity fluid is penetrated by a low-viscosity fluid within a medium where flow is dominated by viscous friction [1] or to "hydraulic fracturing" when a solid (generally a rock) is broken open by injection of a liquid at high pressure [2]. Viscous fingering is an interfacial instability which stems from the destabilizing action of viscous forces, whereas hydraulic fracturing, which can be considered as a subdomain of the more general fracture process [3,4], is a structural instability which is driven by the release of elastic stress. In Newtonian fluids within axial or radial Hele-Shaw cells [1], VF leads to the growth of smooth fingers [5,6], whose width and splitting depend on the capillary number (ratio of viscous over capillary forces). The use of a shear-thinning non-Newtonian fluid introduces an additional instability and allows for a considerable increase of the effective capillary number [7]. This results in a drastic decrease of the wavelength of maximal growth and an increase of branching [8], leading to fractal arborescences [9–11].

One can go a step further with the use of viscoelastic fluids. Viscoelastic fluids are characterized by (at least) one internal relaxation time t_r, which characterizes the time scale of the structural reorganizations within the fluid [12]. It is related to the reciprocal frequencies of the motion of the colloidal particles in the fluid. If the time scale of a flow event, t_{fl}, is much shorter than t_r, the medium responds essentially as an elastic body. In the opposite case, it behaves like a liquid. This can be rationalized in terms of a dimensionless number, $De = t_r/t_{fl}$ [13]. For $De \ll 1$, viscous effects dominate, whereas for $De \gg 1$, the system behaves essentially as an elastic solid. Thus, the use of viscoelastic fluids permits one to think of a possible crossover from fractal growth by flow to fractal growth by fracture by decreasing De. We report here the results of experiments performed with concentrated dispersions of smectite clays [14–16] in water which clearly show the transition between a flow regime characterized by fractal patterns of "fingers" and a fracturing regime characterized by fractal patterns of "cracks." The storage and release of elastic energy in the cell is at the basis of this transition and, as anticipated, the crossover from VF to viscoelastic fracturing (VEF) occurs for a critical value of De.

Our experiments were performed at constant injection flow rate in radial Hele-Shaw cells (two square glass plates of side $2L = 0.45$ m, of thickness e between 4 and 24 mm, separated by a gap $2a = 0.3$ mm), with injection through a 1-mm hole at the center of the bottom plate. The viscoelastic properties of the medium to be invaded were adjusted by increasing the clay/water weight ratio C/W between 0.15 and 0.6. This leads to huge modifications of the rheological parameters with a dramatic increase of the elastic modulus [15,16]. Two low-viscosity Newtonian fluids were injected into the clay suspensions: water ($\mu = 0.89$ mPa s at 298 K) or dodecane ($\mu = 1.35$ mPa s). The interfacial tension between the aqueous colloidal fluid and water is vanishing, whereas it is large in the case of dodecane (0.051 N m^{-1}).

Three sets of experiments were performed. In the first set, only one type of low-deformability cell (12-mm-thick plates) was used while the colloid concentration and the flow rate were varied. In the second set, the concentration and the flow rate were fixed and the cell deformability was changed by varying the plate thickness. In the third set, instead of injecting a fluid under pressure, a given deformation (swelling) rate was applied to the cell by pulling the glass plates apart and allowing air to enter through the injection hole.

Figure 1 shows representative results for the first set of experiments, at constant and low cell deformability. At low flow rate and in a dilute colloidal fluid, the patterns are typical VF patterns [10,11]. The fingers have an essentially rounded profile and the branching angle is much smaller than 90°. Branching occurs at the finger tips. On the other hand, at high flow rates in rigid pastes, the fingers look clearly like cracks. They have a sharp tip. Branching occurs at right angles and, most important, *behind* the tips. In addition, the cracks are generally curved and branching occurs systematically on the convex side of the main crack. These elements show clearly that branching stems from the rise of a tensile stress parallel to the growth direction of the mother cracks.

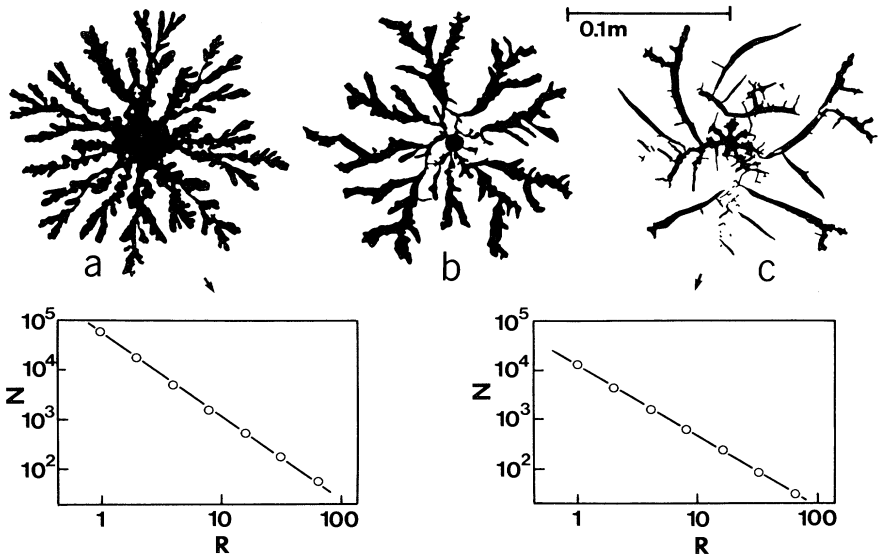

FIG. 1. Patterns obtained by injecting water into water-based smectite muds or pastes. The clay concentration in the colloidal fluid increases from left to right (the clay/water ratios are 0.08, 0.10, and 0.20, respectively). The first pattern is identified as a viscous fingering pattern, and the last pattern as a viscoelastic fracturing pattern. The central pattern is in the crossover regime. The mass fractal dimensions of the first and last patterns, derived by a box-counting method from log(number of occupied boxes) vs log(box size in pixels) plots, are 1.65 and 1.43, respectively.

The morphological differences between VF and VEF patterns can be analyzed in terms of local curvatures along their boundaries. As shown in Fig. 2, VF patterns are characterized by rather smooth convex curvatures (large curvature radii) located at the finger tips and sharp concave curvatures in the bottom of the "fjords." As the VEF regime settles in, the fjords tend to disappear and the amplitude of the convex curvatures sharpens. Deep into the VEF regime, the curvature profiles display large domains of vanishing curvature (the crack walls) and small spots of very large convex curvature (the crack tips).

In spite of these deep modifications, VEF patterns are still mass fractals, like VF patterns, but their mass fractal dimension D_m is systematically lower than what is expected for diffusion-limited-aggregation-type patterns ($D_m \simeq 1.68$) as found for fractal viscous fingering in Hele-Shaw cells [10]. We measured values ranging from 1.6 down to 1.4 ± 0.05, over almost two decades, by a box-counting method. This lower value of D_m is in qualitative agreement with values obtained from simulation studies of crack propagation on bond networks using either deterministic [17] or random [18,19] bond-breaking models. Interfacial tension does not seem to interfere with our results. It merely increases the average crack width.

The large morphological differences between fingering and fracturing patterns permit us to classify a given pattern in either one of these categories without ambiguity. This in turn allows one to construct a fingering-fracturing "phase diagram" in the plane relating the injection flow rate Q to the paste colloid concentration C/W. As shown in Fig. 3, the boundary between the two regimes is roughly hyperbolic. This is in agreement with the idea that the crossover occurs when the reciprocal time of the mechanical excitation, t_{fl}^{-1}, which is expected to vary like Q, exceeds the frequency of the internal relaxation processes, t_r^{-1}, which is expected to vary as $(C/W)^{-1}$ (the stronger the paste, the slower the rate of microscopic rearrangements). In other words, the stronger the paste, the smaller the flow rate necessary to exceed the structural rearrangement rate. Hence, a transition occurring at constant De is equivalent to a transition occurring for a critical flow rate value, $Q_{crit} \sim (C/W)^{-1}$. As shown in Fig. 3,

FIG. 2. Local curvature along the boundaries of the patterns shown in Fig. 1. Positive values correspond to a convex curvature.

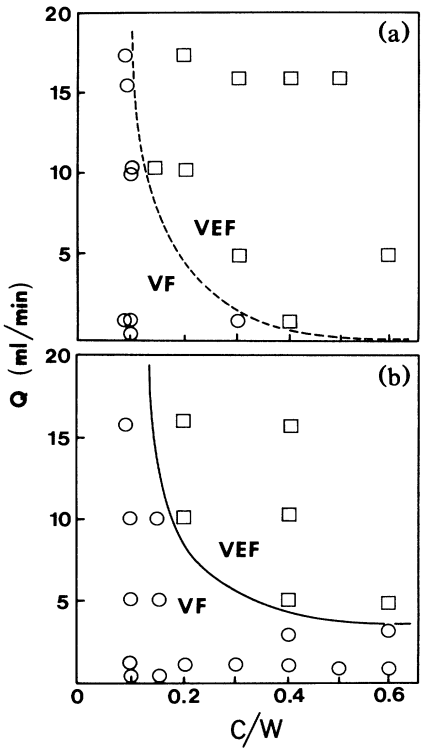

FIG. 3. Viscous fingering (circles) vs viscoelastic fracturing (squares) "phase diagram," in the plane relating the injection flow rate to the colloid concentration: (a) in the miscible and (b) in the immiscible case, respectively.

the interfacial tension merely shifts the boundary between the two regimes towards larger flow rates (higher mechanical frequencies) and stronger pastes (smaller relaxation frequencies).

More precisely, in two series of experiments performed at $C/W=0.2$ and 0.3 (fourteen runs), we were able to measure $t_{fl}=l/U$ on video records, where l is the average finger or crack width and U is the average tip velocity, calculated from the diameter-versus-time curve in the quasilinear regime. We found, without any exception, that, at a given C/W, the type of regime is controlled by t_{fl} indeed. The transition occurs at $t_{fl}=0.3$ s for $C/W=0.2$ and at $t_{fl}=0.2$ s for $C/W=0.3$, which is consistent with $Q_{crit}\sim(C/W)^{-1}$.

In order to quantify the VF-VEF transition, we performed experiments with variable plate thickness. Figure 4 shows that, keeping the flow rate and concentration constant, one also induces the fingering-fracturing transition by increasing the cell deformability, i.e., decreasing e from 24 to 4 mm. In the following, we propose a semiquantitative criterion for each regime, leading to a prediction of the transition.

The creeping motion of a sphere through a plastic fluid has been theoretically studied by Beris *et al.* [20]. Their main result is that the condition for a sphere to move is that the ratio of the driving force for motion (in our case, the pressure gradient $\partial p/\partial\rho$) to the yield stress τ_y has to be higher than a critical value, $\alpha\simeq 7$. In our case the driving force for a bubble of radius R between the two plates separated by a distance $2a$ is of the order of $2aR^2|\partial p/\partial\rho|_{\rho=R}$. If the bubble is inflated at a pressure P, the pressure gradient is $(\partial p/\partial\rho)_{\rho=R}=2P/R$, and the bubble will move at a pressure P_{VF}:

$$P_{VF}=\alpha\tau_y R/2a\,. \tag{1}$$

On the other hand, as a first approximation, we assume that crack opening occurs when the elastic energy stored in the cell deformation exceeds the energy required to overcome the yield stress. This is reminiscent of Griffith's criterion in which the kinetic and cohesive energies have been neglected with respect to energy dissipation, as usual for fracture in viscoelastic media. The elastic energy is of the order of $P\Delta V$, where ΔV is the increase in cell volume due to the plate deformation:

$$P\Delta V\approx\pi Lh^2\,. \tag{2}$$

h, the deformation, is of the order of $P\epsilon^2L^4/Ee^3$, where

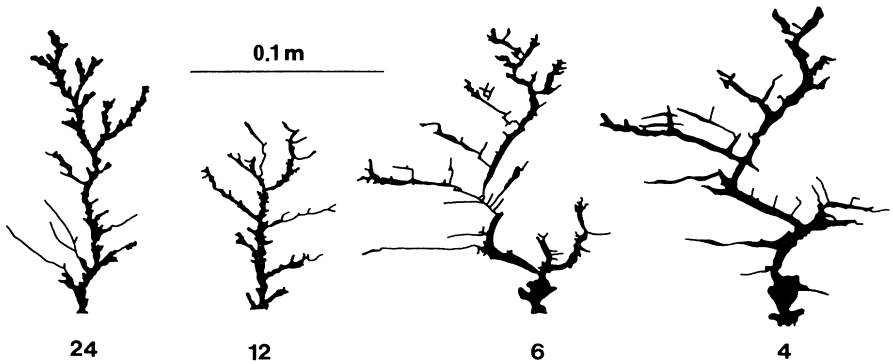

FIG. 4. Patterns obtained at constant paste concentration ($C/W=0.1$) and injection rate ($Q=10$ ml/min) by using Hele-Shaw cells with decreasing plate thickness, from left to right (thickness indicated in mm). Only one of the main branches of the patterns is represented.

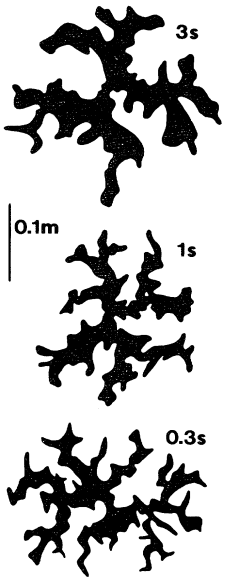

FIG. 5. Patterns obtained at imposed cell deformation rate, at constant paste concentration ($C/W=0.2$). The value of τ_{fl} decreases from top to bottom, as indicated.

ϵL is the radius on which the pressure is applied ($\epsilon \ll 1$) and E is the elastic modulus of the glass. On the other hand, the energy dissipated by displacing the paste a distance $2a$ across the cell is of the order of $\tau_y(2L)^2 2a$. Hence, the critical pressure at which fracturing will be initiated is increasing as

$$P_{VEF} \approx C(e/L)^2, \tag{3}$$

with $C=(\tau_y a E^2/\epsilon^2 L)^{1/3}$. At low plate thickness, P_{VEF} may be smaller than P_{VF}, in which case one expects to initiate fracturing rather than viscous fingering. On the other hand, for thicker plates, P_{VEF} will exceed P_{VF} and one should observe viscous fingering.

Finally, in a third series of experiments performed with a paste at $C/W=0.2$, the glass plates were pulled apart and air was allowed to enter the cell through the injection hole. Figure 5 shows the pattern evolution as the deformation rate, and thus τ_{fl}, increases. Although the morphology of the patterns is not as clearly identified as VEF as previously, due to the large surface tension, one can reasonably recognize the 90° branching regime typical of VEF in the last pattern obtained at $\tau_{fl}=0.3$ s. This latter value is in good agreement with the value observed for the onset of VEF in the constant-concentration–constant-cell-deformability experiments.

One of us (E.L.) is grateful to the Institut Français du Pétrole for financial support.

[a]To whom correspondence should be addressed.

[1] G. M. Homsy, Annu. Rev. Fluid Mech. **19**, 271 (1987).
[2] D. Mader, *Hydraulic Proppant Fracturing and Gravel Packing* (Elsevier, Amsterdam, 1989).
[3] *Statistical Models for the Fracture of Disordered Media,* edited by H. J. Herrmann and S. Roux (North-Holland, Amsterdam, 1990).
[4] *Disorder and Fracture,* edited by J. C. Charmet, S. Roux, and E. Guyon, NATO Advanced Study Institutes, Ser. B, Vol. 235 (Plenum, New York, 1990).
[5] P. G. Saffman and G. I. Taylor, Proc. Roy. Soc. London A **245**, 312 (1958).
[6] L. Paterson, J. Fluid Mech. **113**, 513 (1981).
[7] H. Van Damme, E. Alsac, C. Laroche, and L. Gatineau, Europhys. Lett. **5**, 25 (1988).
[8] H. Van Damme, E. Alsac, and C. Laroche, C. R. Acad. Sci. **309**, Ser. II, 11 (1989).
[9] J. Nittmann, G. Daccord, and H. E. Stanley, Nature (London) **314**, 141 (1985).
[10] G. Daccord, J. Nittmann, and H. E. Stanley, Phys. Rev. Lett. **56**, 336 (1986).
[11] H. Van Damme, C. Laroche, P. Levitz, L. Gatineau, and C. Laroche, Nature (London) **320**, 731 (1986).
[12] R. B. Bird, R. C. Armstrong, and O. Hassager, *Dynamics of Polymeric Liquids* (Wiley, New York, 1987), Vol. 1.
[13] M. Reiner, Phys. Today **17**, 62 (1964).
[14] Smectite clays are colloidal minerals with a layered crystal structure, often referred to as "swelling clays" [see, for instance, H. van Olphen, *Introduction to Clay Colloid Chemistry* (Wiley, New York, 1978)]. The most important member of the family is montmorillonite, which is commercially available under the name bentonite. We used FTP3 grade bentonite, from CECA S.A., Paris.
[15] H. Van Damme, C. Laroche, and L. Gatineau, Rev. Phys. Appl. (Paris) **22**, 241 (1987).
[16] H. Van Damme, C. Laroche, L. Gatineau, and P. Levitz, J. Phys. (Paris) **48**, 1121 (1987).
[17] H. J. Herrmann, J. Kertesz, and L. De Arcangelis, Europhys. Lett. **10**, 147 (1989).
[18] E. L. Hinrichsen, A. Hansen, and S. Roux, Europhys. Lett. **8**, 1 (1989).
[19] P. Meakin, G. Li, L. M. Sander, E. Louis, and F. Guinea, J. Phys. A **22**, 1393 (1989).
[20] A. N. Beris, J. A. Tsamopoulos, R. C. Armstrong, and R. A. Brown, J. Fluid Mech. **158**, 219 (1985); for a review, see R. P. Chhabra and P. H. T. Uhlherr, in *Encyclopedia of Fluid Mechanics,* edited by N. P. Cheremisinoff (Gulf, Houston, 1988), Vol. 7, Chap. 21.